

23 **Abstract**

24 The diversification or decoupling of production chains from China to alternative Asian countries
25 such as India or Indonesia would impact the spatial distribution of anthropogenic emissions, with
26 corresponding economic impacts due to mortality associated with particulate matter exposure. We
27 evaluated these changes using the Community Earth System Model, the Integrated Exposure-
28 Response (IER) model and Willingness To Pay (WTP) method. Significant effects on PM_{2.5} related
29 mortality and economic cost for these deaths were seen in many East, Southeast and South Asian
30 countries, particularly those immediately downwind of these three countries. Transferring all of
31 export-related manufacturing to Indonesia resulted in significant mortality decreases in China and
32 South Korea by 78k (5 per 100k) and 1k (2 per 100k) respectively, while Indonesia's mortality
33 significantly increased (73.7k; 29 per 100k), as well as India, Pakistan and Nepal. When
34 production was transferred to India, mortality rates in East Asia show similar changes to the
35 Indonesian scenario, while mortalities in India increased dramatically (87.9k; 6 per 100k), and
36 mortalities in many neighbors of India were also severely increased. Nevertheless, the economic
37 costs for these deaths were much smaller than national GDP changes in China (0.9% of GDP vs.
38 18.3% of GDP), India (2.7% of GDP vs. 84.3% of GDP) or Indonesia (9.4% of GDP vs. 337% of
39 GDP) due to shifting all of export-related production lines from China to India or Indonesia.
40 Morally, part of the benefits of economic activity should be used to compensate the neighboring
41 communities where mortality increases occur.

42

43 **Plain Language Summary**

44 An Earth System Model was used to simulate responses of PM_{2.5} to hypothetical manufacturing
45 shift from China to Indonesia or India. Then an Integrated Exposure-Response (IER) model and
46 Willingness To Pay (WTP) method were used to assess impacts on attributable mortality for PM_{2.5}
47 and the corresponding economic costs. Our results show that mortality and economic cost were
48 affected significantly in East, Southeast and South Asian countries. When all of the export-related
49 production was transferred from China to Indonesia, China and South Korea saw significant
50 mortality decreases, while mortalities of Indonesia, India, Pakistan and Nepal increased
51 significantly. When India became the importing country, East Asia showed similar mortality
52 changes to the Indonesian scenario. The biggest increase occurred in India, and other South Asian
53 countries were also affected significantly, with rises for Bangladesh, Bhutan, Nepal and Sri Lanka.

54 Although India and Indonesia need pay the price for significant increases in PM_{2.5} related deaths,
55 these costs were much smaller than national GDP increases due to importing manufacturing. The
56 reduction of China's economic cost due to mortality decreases cannot make up for the larger
57 decline in national GDP. These economic benefits morally should be used to compensate the third
58 countries where mortality increases occur.

59

60 **1 Introduction**

61 The ongoing coronavirus COVID-19 has disrupted global supply, demand and logistics
62 infrastructure (Guan et al., 2020; Ivanov, 2020; Nicola et al., 2020); countries with greater
63 dependency on foreign supply chains have been more negatively affected (Fernandes, 2020). 94%
64 of the Fortune 1000 companies have suffered from interrupted supply chains caused by COVID-
65 19 outbreaks (Sherman, 2020). The resulting material shortages and delivery delays have reduced
66 production, and many multinational businesses have reconsidered their manufacturing
67 deployments (Hayakawa & Mukunoki, 2021; Liu et al., 2020; Free & Hecimovic, 2021). During
68 recent decades, very many international companies have become greatly dependent on Chinese
69 production and supplies, which has increased instability and uncertainties in global trade and
70 supply chains during the COVID-19 pandemic. On July 17, 2020, the Japanese Ministry of
71 Economy, Trade and Industry announced that a first batch of 87 Japanese companies had
72 transferred portions of their supply chain in China to Southeast Asia or back to Japan to reduce the
73 dependence on China. Southeast Asian countries with relatively low labor costs, such as Vietnam,
74 Indonesia and India, are probably the most likely to benefit from a shift of global manufacturing
75 (Lin & Lanng, 2020). In fact, the reshaping of global manufacturing is not only related to epidemic
76 outbreaks, but also the rising risk of trade wars, upward trends in nationalism and protectionism,
77 considerations about sustainability and tackling climate change (Hedwall, 2020; Free &
78 Hecimovic, 2021).

79

80 Many studies have shown that millions of people worldwide die every year from diseases
81 attributed to long-term exposures to fine particulate matter, particularly PM_{2.5} (Brauer et al., 2016;
82 Burnett et al., 2014; Apte et al., 2015; Wang et al., 2018). International trade activities are
83 associated with emissions of air pollutants. Lin et al. (2014; 2016) calculated emissions embodied

84 in export (EEE) of different regions worldwide and analyzed they impacts on atmospheric
85 environment and human health. Zhang et al. (2017) used global emissions, chemistry, trade and
86 exposure models to estimate premature mortality related to PM_{2.5} pollution from the production
87 and consumption process to show that the health impacts of PM_{2.5} attributable to international trade
88 are significant.

89
90 Abrupt reductions in the emission of aerosols and aerosol precursors due to a socio-economic crisis
91 results in immediate and significant global and regional climate responses, while the effects of
92 CO₂ emission reductions are much smaller in the short term (Ran et al., 2021). Other studies have
93 also found that atmospheric CO₂ concentration and its impact on climate due to carbon transfer
94 are very small and lie within observed interannual variability (Wei et al., 2016; Lin et al., 2016).
95 Hence in our simulations, we only change aerosol and aerosol-precursor emissions. The scenarios
96 used simulate moving half, or all, export-related manufacturing from China to either Indonesia or
97 India. This is not a study of the health and economic impacts implied by the COVID-19 pandemic,
98 but rather a study of the potential responses to that might be stimulated by unexpected sudden
99 global or regional economic events. While this study can be seen as a purely hypothetical
100 sensitivity study, it is also of interest given the global redistribution of manufacturing towards the
101 global South.

102
103 We explore the potential risks and benefits to human health and social economy of reshaping
104 global manufacturing, via a series of sensitivity experiments using an earth system model (ESM).
105 We redistributed anthropogenic emissions of aerosols and their precursors from the industry,
106 energy and transportation sectors to represent manufacturing shift from China to Indonesia or India
107 and use these emissions within the ESM to determine changes in surface PM_{2.5}. We then consider
108 PM_{2.5} related mortality from five major diseases, and a widely used metric to monetize attributable
109 mortality and assess economic aspects of transferring manufacturing.

110
111 **2 Methods**

112

113 **2.1 Model**

114 A baseline and four sensitivity simulations were done with the Community Earth System Model
115 version 1.2.2 (Hurrell et al., 2013). The baseline experiment was the B_2000_CAM5_CN
116 component set, including the Community Atmosphere Model 5 (CAM5) (Neale et al., 2010),
117 Parallel Ocean Program version 2 (POP2), Community Land Surface Model (CLM) version 4.0,
118 the Los Alamos sea ice model (CICE) version 4, all coupled together using the CESM coupler
119 CPL7. The horizontal resolution of CAM5 and CLM was $0.9^\circ \times 1.25^\circ$ latitude-longitude (f09 grid),
120 while that of POP2 and CICE was about 1° (g1v6 grid). The vertical coordinate of CAM5 was a
121 hybrid sigma-pressure system consisting of 30 vertical levels, with model top at about 3.6 hPa.
122 CLM had 15 soil layers to 35 m depth, POP2 had 60 height layers, and CICE had five thickness
123 categories.

124

125 The simulations were run with the Modal Aerosol Module with three modes (MAM3). An
126 alternative and more sophisticated seven mode version (MAM7) has been shown to be generally
127 well reproduced by MAM3 (Liu et al., 2012), and so we use the default MAM3 option in
128 B_2000_CAM5_CN. Emissions were based on AeroCom (Aerosol Comparisons between
129 Observations and Models; Textor et al., 2005), although ammonia was prescribed by sulfate in the
130 simplified chemistry of MAM3. Anthropogenic primary black carbon (BC), primary organic
131 matter (POM), sulfur dioxide (SO₂), primary sulfate aerosol and semi-volatile organic gas species
132 (SOAG) were emitted in seven sectors -- agriculture, waste, domestic, energy, industry,
133 transportation, shipping.

134

135 **2.2 Experiment design**

136 The default CESM experiment "B_2000_CAM5_CN" with greenhouse gas (GHG) levels and
137 aerosol emissions of the year 2000 was adjusted to create our "B_2020_CAM5_CN" baseline
138 experiment. The atmospheric GHGs concentrations were updated to that of year 2020 based on
139 NOAA (available at <https://gml.noaa.gov/ccgg/trends/>). The aerosol emissions were replaced with
140 year 2020 values from the Representative Concentration Pathway 6.0 (RCP6.0) scenario
141 experiment in CESM. The RCP6.0 was created for the 5th Climate Model Intercomparison Project
142 (CMIP5) (Taylor et al., 2012), as an intermediate stabilization emission scenario leading to 6.0
143 Wm^{-2} increase in radiative forcing by the end of the century (Moss et al., 2010). Since there is no

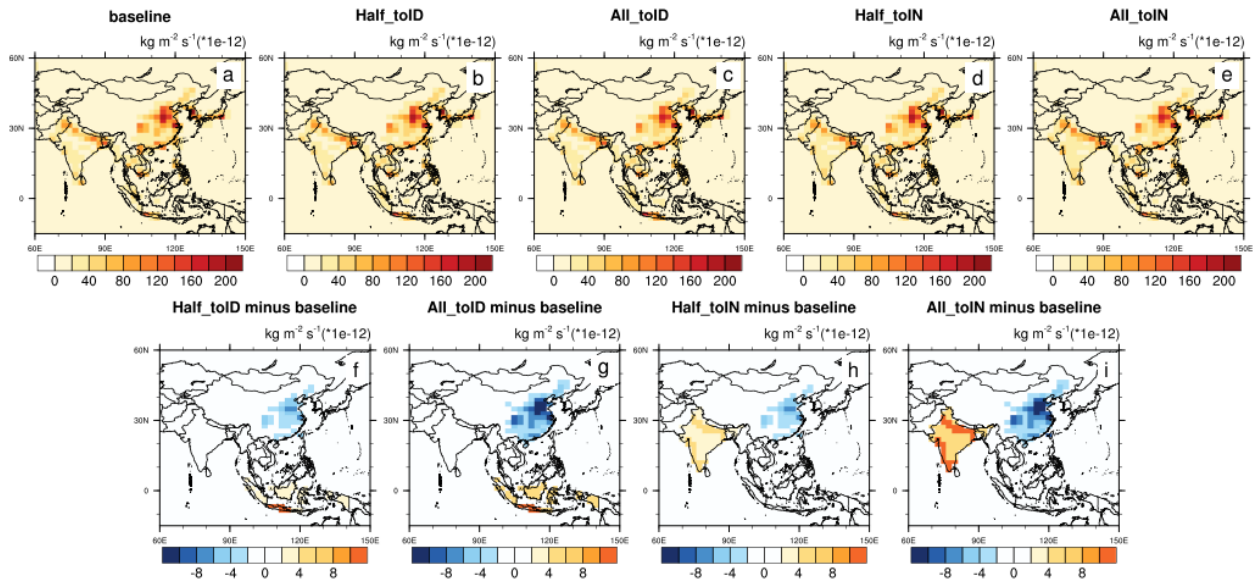
144 significant difference in emissions and temperatures under any scenario around 2020 (Ran et al,
145 2021 and IPCC, 2014), the choice of RCP scenario is not important in our simulations. The
146 “B_2020_CAM5_CN” was run for 200 years to reach the climate equilibrium state of 2020 (Fig.
147 S1.1), and the following analysis for simulation results was based on the median climate state for
148 the third 100 years.

149
150 We redistributed anthropogenic BC, POM, SO₂, primary sulfate aerosol and SOAG emissions in
151 the industry, energy, and transportation sectors to represent manufacturing shifts from China to
152 Indonesia or India. Emissions Embodied in Exports (EEE) was calculated using an Input-output
153 Model (Lin et al., 2016) to determine the proportion of emission transfer in the industry, energy
154 and transportation sectors of China. We integrated the emission sectors described by National
155 Bureau of Statistics of China (NBSC) to meet the classification of emission sectors in CESM (see
156 Table S1.2). The input-output table for 2017 was used because it is the latest available (NBSC,
157 2017). The total merchandise exports and imports in China changed little between 2017 and 2020
158 (Fig. S1.2). Other economic data needed for the calculation was also derived from NBSC. Results
159 show that EEE of China in industry, energy, and transport sector accounts for about 22.4%, 17.9%
160 and 23.8% of total emissions, respectively.

161
162 We created four sensitivity simulations for detecting a response of the climate system to
163 manufacturing redistributions based on the climatic equilibrium state of the baseline experiment
164 (Table S1.1). These are, i) All_toID: all of China EEE transferred to Indonesia; ii) Half_toID: half
165 of China EEE transferred to Indonesia; iii) All_toIN: all of China EEE transferred to India; iv)
166 Half_toIN: half of China EEE of transferred to India. Available labor is generally proportional to
167 population density, so we distributed the EEE of China around Indonesia or India based on the
168 geographic population distribution in 2020 (Fig. S1.3) rather than evenly increasing emissions
169 across Indonesia or India (Figure 1).

170

Annual mean aerosol emissions in 2020



171 **Figure 1.** Annual mean total anthropogenic aerosol and aerosol precursor emissions ($10^{-12} \text{ kg m}^{-2}$
 172 s^{-1}) for the baseline and the four sensitivity simulations for the year 2020, and the differences
 173 between them. Here is the hypothetical aerosol mass emission, described as the sum of BC, POM,
 174 primary sulfate aerosol, sulfate and SOA emission. Sulfate and SOA here refer to the part of SO_2
 175 and SOAG that has been converted to sulfate or SOA.
 176
 177

178 **2.3. Correction for Modeled $\text{PM}_{2.5}$**

179 We compared the simulated 100-year mean $\text{PM}_{2.5}$ concentrations in our baseline run with $\text{PM}_{2.5}$
 180 concentrations for 2010-2020 at $0.1^\circ \times 0.1^\circ$ horizontal resolution given by van Donkelaar et al.
 181 (2021) of combined satellite observations, chemical transport modeling and ground-based
 182 monitoring. The distribution of $\text{PM}_{2.5}$ concentrations in the baseline was similar to that of the
 183 satellite-derived $\text{PM}_{2.5}$ (van Donkelaar et al., 2021), but with significant differences in some areas
 184 of interest in this study (China, India and Indonesia), and further afield over West Asia and North
 185 Africa (Fig. S2.1). Since ammonia is not directly simulated in the MAM3 aerosol module,
 186 ammonium sulphate is effectively prescribed. We performed the baseline experiment with the
 187 computationally more expensive MAM7 module for year 2000, which explicitly simulated
 188 ammonia, and which improved $\text{PM}_{2.5}$ concentrations over the Indian subcontinent and North China,
 189 but not over Indonesia and Southeast Asia (Fig. S2.2). Therefore, we do not consider the use of
 190 MAM3 rather than MAM7 as the main reason for the $\text{PM}_{2.5}$ deficiencies.

191

192 The multi-year average surface concentrations of each simulated aerosols (with diameters less than
193 2.5 μm) in the baseline has similar spatial distribution as the 2010-2020 average from Modern-Era
194 Retrospective analysis for Research and Applications version 2 (MERRA-2; GMAO, 2015; Fig.
195 S2.3). However, sulfate and POM in the baseline were significantly underestimated across much
196 of Asia, particularly North India, East China and for the island of Java. The most plausible reason
197 is that the emission inventory used by MAM3 did not capture the high emissions of anthropogenic
198 sulfur dioxide and organic carbon emissions in regions where sulfate and POM was severely
199 underestimated. Sea salt and dust showed some differences, but are not affected by transfer of
200 manufacturing (Fig. S2.4 and S2.5). In fact, the $\text{PM}_{2.5}$ bias outside East Asia, South Asia and
201 Southeast Asia, had little effect on our results, as $\text{PM}_{2.5}$ concentrations and $\text{PM}_{2.5}$ related mortality
202 outside Asia did not change significantly in our simulations (Fig. S3.1 and Fig. S3.2).

203

204 Because of the health impacts of $\text{PM}_{2.5}$ scale non-linearly with concentration – that is the same
205 increase in concentration has larger impacts when added to a low concentration background than
206 it does on a high concentration one, we need to correct simulated $\text{PM}_{2.5}$ in Asia with reanalysis
207 data and observed data. Firstly, we corrected modelled sulfate, BC, POM, dust and sea salt aerosol
208 concentrations (only considering aerosols less than 2.5 μm in diameter) in Asia, by multiplying
209 them by the ratio of each aerosol concentration in MERRA-2 to that in the baseline ($0.9^\circ \times 1.25^\circ$;
210 Fig. S2.3). The weighted sum of the five aerosols and secondary organic aerosol (SOA) represents
211 the simulated $\text{PM}_{2.5}$ concentration (Eq. 1). The weight for each aerosol was found by multiple
212 linear regression (MLR) between aerosols and the satellite-derived $\text{PM}_{2.5}$ from van Donkelaar et
213 al. (2021). Particular aerosols in various countries are highly correlated (we took $R > 0.85$ here;
214 Sheet 1 in Supplementary Excel 1), so, for that country we combined the highly correlated aerosols
215 into a single variable (Sheet 2 of Supplementary Excel 1) for the MLR to avoid issues with over-
216 fitting. The same procedure was applied for $\text{PM}_{2.5}$ in all experiments, and the subsequent
217 calculations and analysis are based on the corrected $\text{PM}_{2.5}$ concentrations.

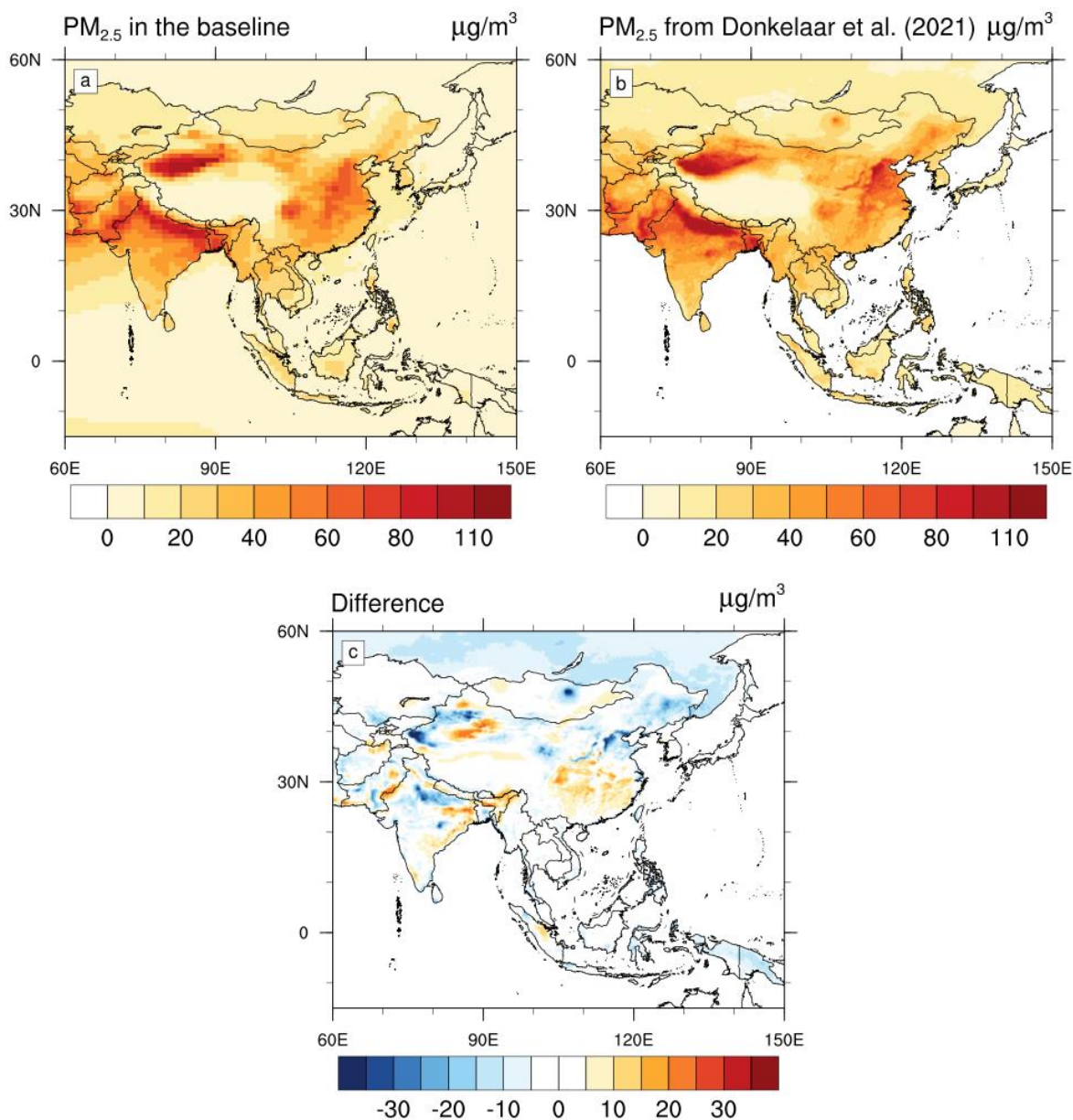
$$218 \quad \text{PM}_{2.5,i(r)} = \sum_{g=1}^6 \text{Aerosol}_{g,i(r)} \times W_{g,r} \quad (1)$$

219 Here, $\text{PM}_{2.5,i(r)}$ is the corrected $\text{PM}_{2.5}$ concentration of grid cell i located in Asian country r .
220 $\text{Aerosol}_{g,i(r)}$ represents the concentration of Aerosol g corrected by MERRA-2 data. $W_{g,r}$ is the
221 regression coefficient for aerosol g in country r .

222

223 The corrected spatial distribution of 100-year mean surface PM_{2.5} concentrations in the baseline
224 simulation is compared with 2010-2020 mean satellite-derived PM_{2.5} (van Donkelaar et al., 2021)
225 in Fig. 2. The high emissions in the North China and the Indo-Gangetic plains were well
226 reproduced. Corrected regional mean PM_{2.5} concentrations of most Asian countries were within
227 20% of observations (van Donkelaar et al., 2021), and within the 95% confidence intervals of the
228 medians (Supplementary Excel 2). Despite clear differences in some places we consider that
229 baseline simulation satisfactorily reproduced the mean present surface PM_{2.5} concentrations and
230 can be used to estimate related mortality and economic costs in our hypothetical cases.

231



233
 234 **Figure 2.** Multi-year mean surface $PM_{2.5}$ concentrations for (a) the baseline simulation with
 235 horizontal resolution $0.9^\circ \times 1.25^\circ$ over the third 100 years (after bias correction), and (b) van
 236 Donkelaar et al. (2021) with horizontal resolution $0.1^\circ \times 0.1^\circ$ over 2010-2020. The differences
 237 (model- van Donkelaar et al., (2021)) between them are shown in (c).
 238

239 **2.4 Calculation of $PM_{2.5}$ related mortality**

240 We considered the five major disease endpoints of $PM_{2.5}$ related mortality where surface $PM_{2.5}$
 241 concentrations are considered a risk factor in the Global Burden of Disease (GBD) 2010 (Global
 242 Burden of Disease Collaborative Network, 2013). For adults (age ≥ 25), these endpoints are

243 ischemic heart disease, cerebrovascular disease (stroke), chronic obstructive pulmonary disease,
244 and lung cancer, and for children under 5, acute respiratory lung infection.

245

246 **2.4.1. Input data**

247 *Global PM_{2.5} and Population Surfaces.* We simulated global annual-average ambient PM_{2.5}
248 concentrations at 1° grid resolution using CESM 1.2.2. We used the global 30 km gridded
249 population data set (Center for International Earth Science Information Network - CIESIN -
250 Columbia University, 2018) of 2020 population in our mortality model, with the PM_{2.5}
251 concentrations interpolated to the same grid using areal conservative remapping.

252

253 *Mortality Data.* We obtained the cause-specific mortalities for the five endpoints in 2019 from the
254 GBD 2019 - the most recent publicly available data set at the Institute for Health Metrics and
255 Evaluation (IHME). Deaths per 100,000 population in 2019 for the five endpoints in 54 countries
256 and three regions are provided in the Supplementary Excel 3.

257

258 **2.4.2 The Concentration-Response function.**

259 The Concentration-Response (C-R) function is a mathematical equation that describes the
260 relationship between exposures to PM_{2.5} and the relative risk of mortality for each endpoint. Here,
261 we employed the integrated exposure-response functions (IERs) (Burnett et al., 2014) to constrain
262 the shape of the C-R relationship and estimate relative risks attributed to PM_{2.5} exposure for the
263 five endpoints. The IER framework parametrizes the dependence of relative risk, RR, on
264 concentration, C (Burnett, 2014):

265

$$\begin{aligned} \text{RR}(C) &= 1 + \alpha [1 - \exp(-\gamma(C - C_0)^\delta)] \quad \text{for } C > C_0 \\ \text{RR} &= 1 \quad \text{for } C \leq C_0 \quad (2.1) \end{aligned}$$

268

269 For each endpoint, C₀ represents a theoretical minimum-risk concentration above which there is
270 evidence indicating health benefits of PM_{2.5} exposure reductions, and parameters α , γ , and δ
271 determine the overall shape of the concentration-response relationship. A distribution of 1000
272 estimates of these parameters for each endpoint for all ages were provided in GBD 2010 (Global
273 Burden of Disease Collaborative Network, 2013). Here we use the median value of the RR from

274 the 1000-member parameter set found over PM_{2.5} concentrations from 0–200 µg/m³ at 0.1 µg/m³
275 steps (see Supplementary Excel 4).

276

277 **2.4.3 Modeling of PM_{2.5} related mortality.**

278 We estimated the premature mortality $M_{i(r),k}$ of all ages for disease endpoint k attributable to
279 ambient PM_{2.5} for grid cell i located in region r (see Equation 2.2). $\hat{I}_{r,k}$ represents the hypothetical
280 “underlying incidence” (i.e., cause-specific mortality rate) for endpoint k that would remain for
281 region r if PM_{2.5} concentrations were reduced to the theoretical minimum risk concentration
282 throughout that region.

283

$$284 \quad M_{i(r),k} = P_{i(r)} \times \hat{I}_{r,k} \times (RR_k(C_{i(r)}) - 1)/100000 \quad \text{where } \hat{I}_{r,k} = \frac{I_{r,k}}{\overline{RR}_{r,k}} \quad (2.2)$$

285

286 Here, $P_{i(r)}$ is the population of grid cell i located in region r , $I_{r,k}$ is the reported regional average
287 annual deaths (per 100,000) for endpoint k in region r , $C_{i(r)}$ represents the annual-average PM_{2.5}
288 concentration in cell i , $RR_k(C_{i(r)})$ is the relative risk for end point k at concentration $C_{i(r)}$, and
289 $\overline{RR}_{r,k}$, as defined below (Equation 2.3), represents the average population-weighted relative risk
290 for end point k within region r :

291

$$292 \quad \overline{RR}_{r,k} = \frac{\sum_{i=1}^N P_{i(r)} \times RR_k(C_{i(r)})}{\sum_{i=1}^N P_{i(r)}} \quad (2.3)$$

293

294 In addition to the absolute number of premature deaths related to PM_{2.5}, we also calculated the per-
295 capita mortality (Equation 2.4) to eliminate the influence of population density.

296

$$297 \quad \overline{M}_{i(r),k} = \frac{M_{i(r),k} \times 100000}{P_{i(r)}} \quad (2.4)$$

298

299 $\overline{M}_{i(r),k}$ is the per-capita attributable mortality for grid cell i located in region r .

300

301 **2.5 Economic assessment**

302

303 **2.5.1 Economic cost for mortality**

304 We used the Value of Statistical Life (VSL), the most generally used metric to monetize
305 attributable mortality for PM_{2.5} (OECD, 2012; OECD, 2014; OECD, 2017; Lu et al., 2017;
306 Giannadaki et al., 2018), to evaluate the economic cost attributed to PM_{2.5} related mortality due to
307 manufacturing transfer. The VSL is the marginal value of a reduction in the risk of dying, and is
308 therefore defined as the rate at which the people are prepared to trade off income for risk reduction
309 (Braathen et al., 2009):

310

$$311 \quad VSL = \frac{\partial WTP}{\Delta R} \quad (3.1)$$

312

313 where R is the risk of dying and ∂WTP is an individual's "Willingness To Pay" to reduce mortality
314 risk by ΔR . VSL is an integration of individual values for small changes in mortality risk, rather
315 that the value of a certain person's life (OECD, 2012).

316

317 We derived the VSL value in constant 2015 USD of PPP (purchasing power parity) terms for the
318 individual countries or regions (OECD Statistics, 2020; see Table S4) for the year 2019 (the latest
319 data available). The total economic cost in country/region r for the year Y can be assessed by
320 multiplying the total number of PM_{2.5} related deaths in country/region r $\sum_{i=1}^N M_{i(r)}$ with the
321 corresponding $VSL_{r,Y}$,

322

$$323 \quad \text{Economic Cost} = \sum_{i=1}^N M_{i(r)} \times VSL_{r,Y} \quad (3.2)$$

324

325 **2.5.2 Economic benefits from additional production**

326 Simple estimation for potential economic changes to Gross Domestic Product (GDP) due to the
327 shift of production lines comes from CO₂ per GDP in China, Indonesia and India (Andrew et al.,
328 2020; BP, 2020), was found using equation (4).

329

$$330 \quad \text{Economic benefits} = \Delta E_r / F_r \quad (4)$$

331

332 Where ΔE_r is the emission change in country r , and F_r refers to CO₂ emissions per GDP in country
333 r .

334

335 **2.6 Uncertainty and significance test**

336 For each experiment, we calculate yearly mortality rate per 30×30 km grid cell based on annual
337 mean PM_{2.5} for 100 years (in the climate equilibrium state), then the 100 estimates for mortality
338 differences between the baseline and sensitivity simulations are calculated for each grid cell and
339 their median values are shown in Figure 4. For an individual country, we consider the sum of
340 mortality rate in each grid cell as national total mortality rate, then deaths per 100k are calculated
341 as the per-capita mortality of this country. One hundred estimates of national per-capita and total
342 mortality and their changes due to manufacturing shift are calculated for each Asian country, and
343 we use the 2.5 and 97.5 percentiles of the 100 estimates as the ranges of mortality rates and their
344 changes (Supplementary Excel 5 and 6). In addition, statements about whether changes in national
345 mortality are significant were evaluated with the non-parametric Wilcoxon signed-rank test for
346 each Asian country (Supplementary Excel 5 and 6). The two-tailed test was carried out at the 0.05
347 significance level.

348

349 For 100-year estimates of national total mortality rates, we calculate corresponding attributable
350 economic cost for mortality using Equation 3.2. Then we use the same method as for mortality to
351 obtain the uncertainty and perform the significance test for economic costs of each Asian country
352 (Supplementary Excel 7).

353

354 **3. Results**

355

356 **3.1 Changes in PM_{2.5} Concentrations**

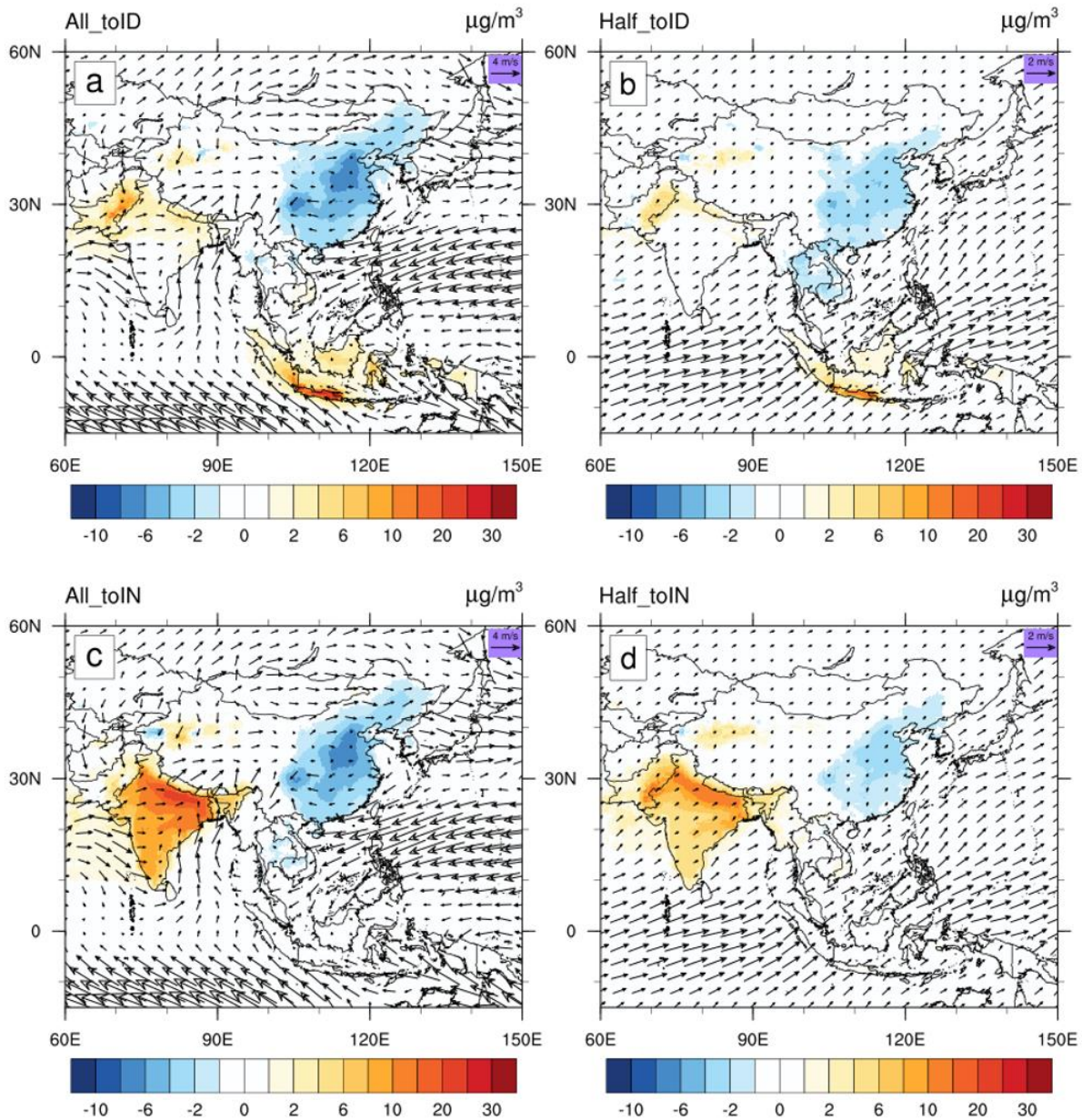
357 As expected, the shift of manufacturing from China to India/Indonesia would result in significant
358 changes in surface PM_{2.5} concentrations in China, India and Indonesia (Fig. 3). When half or all
359 of export-related production lines were transferred to Indonesia, northern China's PM_{2.5}
360 concentrations declined by over 4 $\mu\text{g m}^{-3}$, with local differences much higher than country means
361 (Table 1). PM_{2.5} declines can be also seen in other East and Southeast Asian countries, such as the
362 Korean Peninsula (All_toID), Thailand, Laos, Cambodia, and Vietnam (Half_toID). Transferring

363 industry to Indonesia raised local $PM_{2.5}$, especially in Java Island with rises over $10 \mu\text{g m}^{-3}$, while
364 the country mean increased by about 6.1 or $2.6 \mu\text{g m}^{-3}$ in scenarios All_toID and Half_toID. $PM_{2.5}$
365 increases also occurred in Pakistan, North India, Nepal, driven by annual mean surface winds
366 blowing from Java Island across the equator towards Northern India (Fig. 3a). In the rest of the
367 world, $PM_{2.5}$ concentrations were almost constant after the shift of manufacturing, although there
368 were small but consistent changes in $PM_{2.5}$ seen in Africa and Central Australia that hint at possible
369 teleconnections to the deserts there (Fig. S3.1a, b).

370
371 Transferring production lines to India had similar impacts on China $PM_{2.5}$ concentrations as with
372 manufacturing shifts to Indonesia (Fig. 3). $PM_{2.5}$ in North Korea and South Korea decreased by
373 around $1 \mu\text{g m}^{-3}$ in scenario All_toIN. Except for slight $PM_{2.5}$ increases in Myanmar, $PM_{2.5}$ changes
374 were not obvious in most southeast Asian countries. As expected, the most significant increases
375 occurred in the Indo-Gangetic Plain, rising by over $10 \mu\text{g m}^{-3}$. $PM_{2.5}$ in countries close to India,
376 such as Pakistan, Nepal, Bhutan and Bangladesh were also affected by the manufacturing shift to
377 India. $PM_{2.5}$ concentrations in other parts of the world were barely affected (Fig. S3.1c, d). The
378 impacts of manufacturing shift on surface $PM_{2.5}$ concentrations were localized to East, South and
379 Southeast Asia because aerosol and aerosol precursor emissions were from the surface and not
380 well-mixed in the whole atmosphere, or even the troposphere. So, shifting manufacturing would
381 affect $PM_{2.5}$ concentrations in countries whose emissions had changed and in their downwind
382 countries.

383

Surface PM_{2.5} Changes & Annual Mean Wind



384
 385 **Figure 3.** The median value of the 100-year changes in annual mean surface PM_{2.5} concentrations
 386 ($0.9^\circ \times 1.25^\circ$, color bar) in the (a) Half_toID, (b) All_toID, (c) Half_toIN, and (d) All_toIN
 387 simulations compared with the baseline experiment. Arrows show mean 100-year annual surface
 388 (the lowest level of the model) wind in panels (a) and (c), and its standard deviation in panels (b)
 389 and (d).

390

391

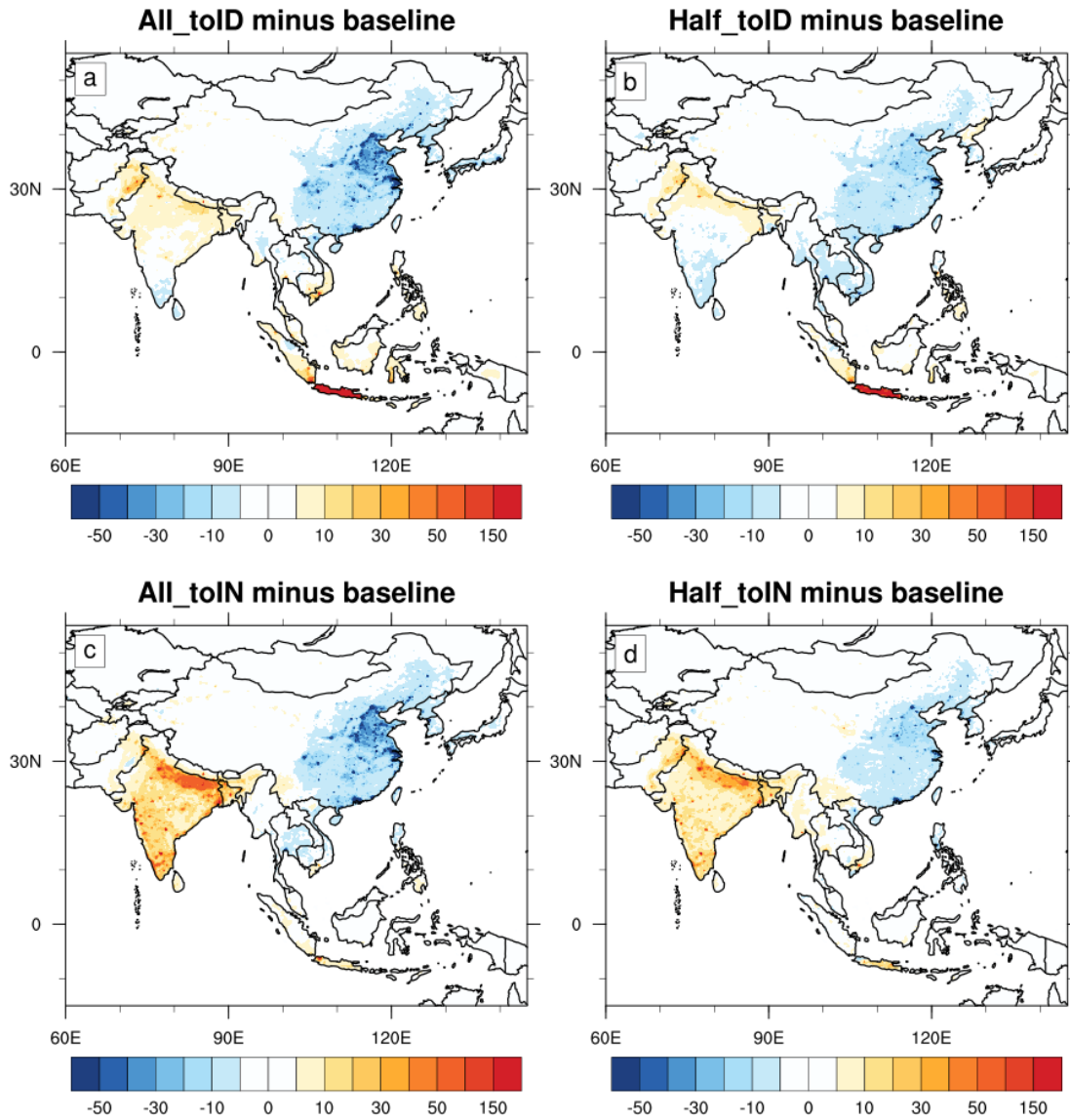
392 **Table 1.** The median value of 100-year regional mean PM_{2.5} concentrations in the baseline at
 393 (0.9°×1.25°) resolution, and the four sensitivity experiments (after bias correction) for China, India
 394 and Indonesia. The numbers in parentheses show the 2.5% and 97.5% percentiles of the
 395 distribution of 100-year regional mean PM_{2.5} concentrations. Unit: µg m⁻³.
 396

	RCP6.0	Half_toID	All_toID	Half_toIN	All_toIN
China	29.9 (27.6-32.8)	29.1 (26.3-31.8)	28.5 (25.6-31.0)	29.4 (26.8-31.5)	28.5 (26.2-31.1)
India	46.3 (41.1-55.3)	47.1 (40.9-55.3)	47.5 (41.5-63.4)	53.4 (46.7-69.8)	56.8 (50.3-68.1)
Indonesia	13.3 (9.9-30.9)	15.9 (12.6-41.7)	19.4 (14.2-47.1)	14.2 (10.3-35.2)	13.7 (10.4-37.5)

397
 398 **Attributable mortality for PM_{2.5}**
 399 We use the abbreviations m for millions and k for thousands of deaths per year. Attributable
 400 mortality for PM_{2.5} in the baseline and the four sensitivity experiments was estimated based on
 401 IERs (Burnett et al., 2014), (Eqn. 2). Giannadaki et al. (2016) applied IERs to evaluate attributable
 402 premature mortality for annual mean PM_{2.5} in 2010. They attributed 3.15m deaths globally in 2010,
 403 with China accounting for 1.33m, followed by India with 575k. China’s attributable mortality for
 404 PM_{2.5} in 2016 estimated by Maji et al. (2018) was 0.96m (with a 95% confidence interval of 0.45
 405 to 1.36m; we use 2.5%–97.5% percentiles as the ranges), accounting for 10.0% of total reported
 406 deaths in China. We estimate PM_{2.5} related mortality in China, India and Indonesia in the baseline
 407 at 1.66m (1.60–1.73 m), 0.99m (0.92–1.07m) and 78k (49–163k; Supplementary Excel 5)
 408 respectively. In most of the regions where PM_{2.5} simulation bias is corrected, our estimates are
 409 comparable to other estimations (OECD Statistics, 2020). China’s mortality rate is overestimated
 410 by 16%, India’s by 1%, and Indonesia’s underestimated by 27% (OECD Statistics, 2020;
 411 Supplementary Excel 5).
 412

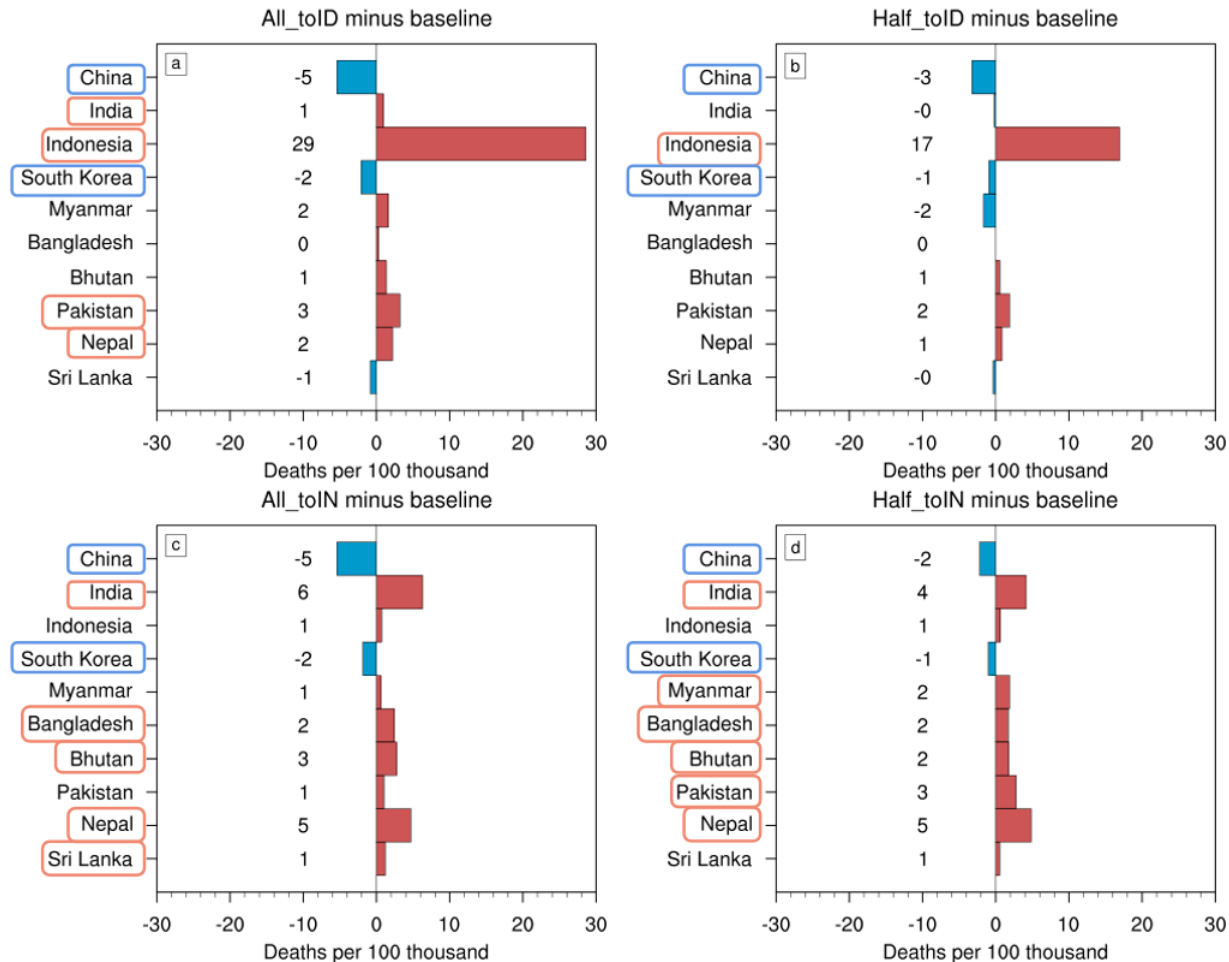
413 Since attributable mortality for PM_{2.5} depends on the population density (which is unchanged by
 414 design in these sensitivity experiments), and PM_{2.5} concentrations (Eqn. 2), its spatial change is
 415 similar to changes in surface PM_{2.5} concentrations (Fig. S3.1 vs. Fig. S3.2; Fig. 3 vs. Fig. 4).
 416 Outside East, Southeast and South Asia there are only insignificant changes in attributable
 417 mortality due to the manufacturing shifts (Fig. 4, Fig. S3.2).
 418

Attributable Mortality for PM_{2.5} (deaths per year)



419
420 **Figure 4.** The median of 100-year estimates of differences of attributable mortality rate per 30×30
421 km grid cell for annual mean surface PM_{2.5} between the four sensitivity simulations and the
422 baseline.
423

Changes in PM_{2.5} related deaths per 100 thousand people



424
 425 **Figure 5.** The median value of 100 estimates of changes in yearly PM_{2.5} related deaths per 100,000
 426 people (see Method 2.6) due to (a) half of China's Emissions Embodied in Exports (EEE)
 427 transferred to Indonesia, (b) all of China's EEE transferred to Indonesia, (c) half of China's EEE
 428 transferred to India, and (d) all of China's EEE transferred to India. Countries boxed in red/blue
 429 have statistically significant increases/decreases in mortality under the two-tailed Wilcoxon signed
 430 rank test at 0.05 significance level. Total mortality rates for these countries are shown in Fig S3.3.
 431

432 Transferring all of export-related production lines into Indonesia (scenario All_toID) resulted in
 433 more significant mortality changes over Asia, compared with scenario Half_toID (Fig. 4a vs. 4b).
 434 China's per-capita mortality attributed to PM_{2.5} decreased dramatically by around 5 deaths per
 435 100k and total mortality by 78k, with the largest decline in North China, while they dropped by 3
 436 per 100k and 46.9k in total under the Half_toID simulation. Significant declines in per-capita and
 437 total mortality can also be seen in South Korea, by 2 per 100k and 1k in total in the All_toID
 438 simulation, and by 1 per 100k and 0.4k in the Half_toID simulation. In the All_toID, mortality

439 reductions can be seen in North Korea and Southern Japan (Fig. 4a), while national total deaths of
440 the two countries changed insignificantly at 0.05 significance level. More modest and less
441 significant declines are simulated in East Asian countries in the Half_toID simulation (see
442 Supplementary Excel 4). In both Half_toID and All_toID scenarios, mortality increased most in
443 Indonesia and with similar patterns, with per-capita and total mortality rising by 29 per 100k and
444 73.7k, and by 17 per 100k and 43.6k respectively. In the wider Southeast Asia region, there were
445 less obvious changes in mortality. Mortality rates in the Indo-Gangetic Plain rose significantly in
446 India (by 1 per 100k or 13.6k), Pakistan (by 3 per 100k or 7.3k) and Nepal (by 2 per 100k or 0.9k)
447 in the All_toID simulation. However, mortality rates in South Asia showed insignificant changes
448 in the Half_toID simulation.

449
450 When all or half of the production lines were transferred to India (All_toIN and Half_toIN
451 scenario), changes in attributable mortality for PM_{2.5} in East Asia were quite similar to the
452 Indonesian scenario (Fig. 4). Significant decreases in mortality rate were simulated for China and
453 South Korea (Fig. 5c and 5d). However, in the Half_toID simulation, the declines in China's
454 mortality rates were smaller than that in Half_toIN, and slight increases can be seen in Yunnan
455 Province, China. In Southeast Asia, increases in mortality rates can be seen in Indonesia,
456 especially in Java, but national per-capita and total mortality were unchanged at the 0.05
457 significance level, except for mortality rate of Myanmar which showed significant increase in the
458 Half_toIN scenario. For India, especially over the Gangetic Plain and the southern tip of the India
459 Peninsula, there would be significant increases, with per-capita and total mortality rates increasing
460 by 6 per 100k and 87.9k under the All_toIN scenario, and by 4 per 100k and 57.8k under Half_toIN.
461 National per-capita and total mortality rates of other South Asian countries were also severely
462 affected in the simulations, with rises under All_toIN for Bangladesh by 2 per 100k and 3.9k,
463 Bhutan by 3 per 100k and 0.04k, Nepal by 5 per 100k and 1.9k, and Sri Lanka by 1 per 100k and
464 0.2k. Pakistan's mortality rate rose under Half_toIN (3 per 100k; 6.4k), while changes were not
465 significant under the All_toIN scenario.

466
467 In conclusion, significant changes in attributable mortality for PM_{2.5} occurred in the three countries
468 whose industries were changed in the simulations. Moreover, many countries downwind also
469 experience significant changes in mortality rates. The differences in significance between All and

470 half scenarios likely represents the importance of extremes in the PM_{2.5} distribution, with 100 years
471 of simulations sometimes not being enough to well define the country 95% confidence intervals.
472 Mortality rates outside the East, South and Southeast Asian region are unaffected in the simulation.

473

474 **3.2 Economic responses assessment**

475

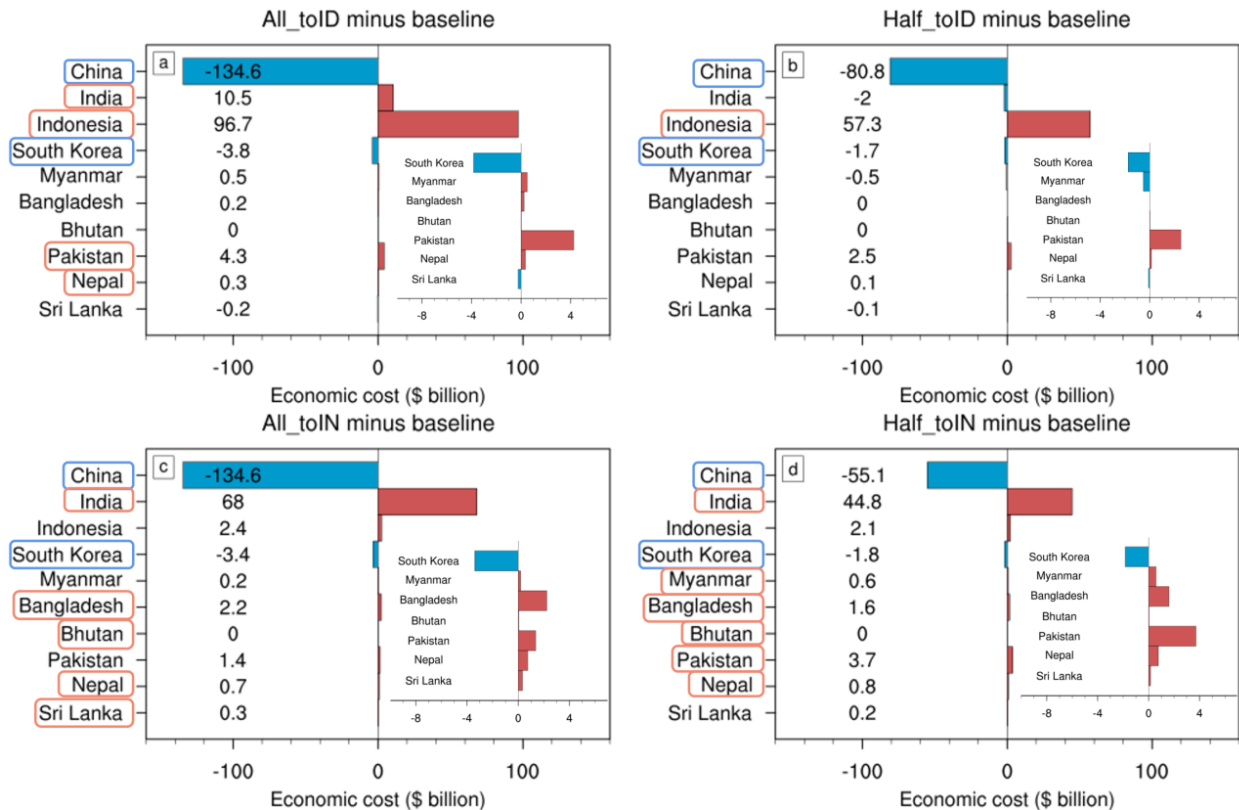
476 We estimated economic costs for individual Asian country in 2020 US dollars (\$) of attributable
477 mortality for PM_{2.5} in the baseline and sensitivity simulations by applying mortality estimates from
478 Eqn. (3.2) (Supplementary Excel 3). The economic cost for a region was based on mortality due
479 to PM_{2.5} pollution and its Willingness To Pay (WTP) to reduce mortality. In the baseline, Chinese
480 economic cost for the 1.66m annual deaths attributed to PM_{2.5} pollution was estimated to be the
481 highest in Asia, about \$2.86 trillion, followed by India (\$0.77 trillion for the 0.99 m annual deaths)
482 and Indonesia (\$0.10 trillion for the 78k annual deaths). Our estimates are in reasonable accordance
483 with other estimates (OECD Statistics, 2020; Supplementary Excel 7) for most of the regions with
484 significant changes in economic cost, but Bangladesh, Bhutan, Myanmar and Nepal are severely
485 overestimated.

486

487 To evaluate the economic impact when China's export-related production lines were transferred
488 to India or Indonesia, we subtracted the baseline economic cost from that in the sensitivity
489 simulations (Fig. 6 and Supplementary Excel 7). As changes in economic costs attributed to PM_{2.5}
490 related mortality were insignificant outside Asia (Supplementary Excel 7), we only focus on the
491 most impacted regions (East, Southeast and South Asia), to analyze the potential economic impact
492 due to manufacturing shift.

493

Changes in attributable economic cost



494 **Figure 6.** The median value of 100 estimates of changes in economic cost of PM_{2.5} related deaths
 495 (\$ billion) due to (a) half of China's Emissions Embodied in Exports (EEE) transferred to Indonesia,
 496 (b) all of China's EEE transferred to Indonesia, (c) half of China's EEE transferred to India, and
 497 (d) all of China's EEE transferred to India. Countries in red/blue box have statistically significant
 498 increases/decreases in economic cost under the two-tailed Wilcoxon signed rank test at 0.05
 499 significance level.
 500

501
 502 When all or half of China's export-related production lines were moved to Indonesia (scenario
 503 All_toID and Half_toID), China had the biggest drop in economic cost by \$134.6 billion
 504 (corresponding to 0.9% of GDP) and \$80.8 billion (corresponding to 0.6% of GDP) respectively.
 505 South Korea also showed significant cost decreases by \$3.8 billion in All_toID and \$1.7 billion in
 506 Half_toID. Indonesia saw the most significant increase in costs, by \$96.7 billion or 9.4 % of GDP
 507 in All_toID, and by \$57.3 billion or 5.6 % of GDP in Half_toID. However, costs of other Southeast
 508 Asian countries also showed insignificant changes when shifting manufacturing to Indonesia. For

509 South Asia, there would be significant cost increases in India, Pakistan and Nepal, by \$10.5 billion,
510 \$4.3 billion and \$0.3 billion respectively if all of production lines were transferred to Indonesia.

511
512 When all of China's export-related production lines were introduced to India (scenario All_toIN),
513 decreases in economic cost of East Asia were more significant than that in Half_toIN. The biggest
514 decreases occurred in China, and the same as for the All_toID scenario, followed by South Korea
515 with cost declines by \$3.4 billion. Changes in the economic costs of South Asia are obvious both
516 in the All_toIN and the Half_toIN simulations. Significant increases were simulated in India's
517 annual costs by \$68 billion (or 2.7% of GDP in 2020) and \$44.8 billion (or 1.8% of GDP in 2020)
518 in All_toIN and Half_toIN respectively, as well as to Bangladesh (\$2.2 billion and \$1.6 billion),
519 and Nepal (\$0.7 billion and \$0.8 billion). The economic cost to Pakistan increases significantly
520 by \$3.7 billion in Half_IN, while that to Sri Lanka rose significantly in All_toIN (by \$0.3 billion).

521
522 Our findings indicated that transferring production lines from China to India or Indonesia
523 contributed to a significant decline in China's attributable economic cost for PM_{2.5} related
524 mortality, and a considerable increase in India or Indonesia's cost. Furthermore, economic costs
525 of other countries were produced as may be expected from the changed PM_{2.5} attributable deaths.
526 Shifting manufacturing to India impacts more countries than shifting to Indonesia. But simulating
527 half of production lines to Indonesia produced the least significant changes.

528
529 Besides the effects on attributable economic costs for PM_{2.5} related mortality, the shift of
530 manufacturing is expected to bring considerable economic benefits to India or Indonesia, as
531 additional production lines can boost local productivity and national GDP. India's CO₂ emissions
532 per GDP is the highest, at 0.91 kg/\$, follows by China and Indonesia, at 0.71 and 0.55
533 kg/\$ respectively. In other words, given the same increase in GDP, Indonesia emits the least CO₂
534 while India emits the most. When all or half of China's export-related production lines were
535 transferred to India, India's GDP increased by \$2091 billion or \$1045 billion, corresponding to
536 84.3% or 42.1% of GDP in 2020, which would be much bigger than India's economic cost due to
537 PM_{2.5} related mortality (corresponding to 2.7% or 1.8% of GDP). Moving all or half of production
538 lines to Indonesia brought an increase by \$3460 billion or \$1730 billion in Indonesian GDP, which
539 corresponded to 337% or 168% of GDP, far outpacing Indonesia's economic cost (corresponding

540 to 9.4% or 5.6% of GDP). However, China's GDP declined by \$2680 billion if all of export-related
541 production lines leave, corresponding to 18.3% of GDP in 2020, which was also much bigger than
542 China's PM_{2.5} attributable economic costs corresponding to 0.9% of GDP. Cost reduction of China
543 was smaller in Half_toIN than Half_toID, but they were both much smaller than reductions in
544 China's GDP.

545

546 **Discussion and Conclusion**

547 The COVID-19 pandemic is reshaping the global trade and supply chains, and some developed
548 countries may consider relocating strategic manufacturing operations out of China, providing new
549 opportunities for some South and Southeast Asian countries. Since the shift of manufacturing is
550 accompanied by redistribution of emission sources of greenhouse gases and aerosols, the impacts
551 on environment and health of the countries directly involved and their neighbors, should also be
552 considered. Since greenhouse gases are well-mixed in the atmosphere, changes in their emission
553 sources have little impact on climate and the environment. Therefore, we only considered changes
554 in PM_{2.5} concentrations due to aerosols and their precursors. We used the Community Earth
555 System Model version 1.2.2 to simulate PM_{2.5} and the socio-economic responses to very large
556 shifts in economic activity. These huge industrial changes and their associated aerosol and their
557 precursor emissions provide sensitivity studies rather than realistic economic scenarios. In fact, it
558 is difficult to quantify the precise changes of emissions worldwide in the process of manufacturing
559 shift.

560

561 Our results indicated that transferring all or half of export production lines from China to India or
562 Indonesia can significantly affect mortality and economic cost attributed to PM_{2.5} changes,
563 especially in China, India and Indonesia, but also in the wider Asian region, especially in the
564 countries downwind of China, Indonesia and India. Shifting manufacturing to India in our
565 simulations led to more Asian countries showing significant changes in PM_{2.5} related deaths and
566 economic costs than an equivalent shift to Indonesia. However, the economic costs of China,
567 Indonesia and India were much smaller than changes in economic benefits due to manufacturing
568 shift. This is of course not the situation for neighboring countries that gain no economic benefit
569 domestically, but suffer (or benefit) from the PM_{2.5} transport.

570

571 In making the mortality estimates, the simple 100-year annual mean surface PM_{2.5} concentrations
572 from the climate model do not fit well to satellite observations, particularly in parts of northern
573 China, northern India and Indonesia, the key areas that we focused on. Since the health impacts of
574 PM_{2.5} scale are non-linearly with concentration, a correction for PM_{2.5} in Asia needed to be done
575 rather than work with simple anomalies in PM_{2.5} relative to the baseline.

576
577 The range of PM_{2.5} related mortality (Fig. 5) in this study was only determined by uncertainties in
578 the CESM-simulated PM_{2.5} concentrations over the 100-year simulations (in the climate
579 equilibrium state) of the present, and so represents the climate model variability in weather and
580 climate. Although we quote 2.5% and 97.5% percentiles of the distribution of 100 estimates as the
581 range of mortality rates, there are other uncertainty sources we do not estimate, such as
582 uncertainties inherent in the relationship between PM_{2.5} exposure and the relative risk of mortality.
583 Other models than the IER type we chose have been used previously to evaluate the relative risk
584 to air pollutant concentrations. Of seven different forms of Concentration-Response functions used
585 previously (Cohen et al., 2004; Pope et al. 2009, 2011), Burnett et al (2014) considered the IER
586 model was a superior predictor of relative risk. Maji et al. (2018) applied an IER and also non-
587 linear power law (NLP; Chowdhury & Dey, 2016) and log-linear (LL; Lelieveld et al., 2013)
588 models to assess PM_{2.5}-related mortality for 338 Chinese cities in 2016. China's total attributable
589 mortality was 9.64 million (IER), 1.258 million (LL) and 0.770 million (NPL). These differences
590 are larger than between the sensitivity scenarios we simulated. However, since we focus on the
591 changes in mortality, the consistent methodology should be sufficient to detect regional and
592 country-by country differences in response. The model resolution for PM_{2.5} and population are
593 also the key factors that can affect the uncertainties of mortality estimates. We interpolated the
594 lower-resolution PM_{2.5} concentrations into the higher-resolution population grid, because
595 industrial emissions of PM_{2.5} are spatially highly variable and closely linked to population.

596
597 The economic cost estimates were based on the 100 estimates of PM_{2.5} related mortality. But there
598 are additional uncertainties from such a monetized assessment of attributable mortality for PM_{2.5}.
599 Country-specific empirical studies on the WTP are lacking, particularly in low- and middle-income
600 countries (Roman et al., 2012; Giannadaki et al., 2018), and thus increase the uncertainties in the
601 estimation of VSL and economic costs. Country-specific VSL in this work came from OECD

602 Statistics (2020) for the year 2019. However, Maji et al. (2018) criticized such an unreasonably
603 high estimate of economic cost in China where the VSL was about \$0.98 million USD for the year
604 2010 (Giannadaki et al., 2018), they believe province-specific VSL is a better method for
605 evaluation of economic costs caused by PM_{2.5} related mortality in China than country-specific
606 VSL.

607
608 This work only considered the potential effects of redistribution of production lines on human
609 health and social economy, but such economic activity may impact regional temperatures and
610 precipitation through the interaction of aerosols and climate, further leading to socio-economic
611 responses. Our analysis shows that, transferring production lines from China to Indonesia would
612 lead to less Asian countries with significant increases in PM_{2.5} related mortality and attributable
613 economic cost than to India. This is because of the maritime Indonesian setting as well as patterns
614 of surface winds. Higher wind standard deviation over the oceans compared with the land (Fig. 3),
615 means that winds disperse PM_{2.5} more widely from Indonesia than India. Perhaps the most
616 concerning aspect of this study is the damage to “innocent” victims of any manufacturing shifts in
617 third countries that do not see any domestic economic gains. Morally the “polluter-pays” principle
618 should be applied and the countries that gain economically from any change in production should
619 provide compensation. In practice that can be done statistically, but attributing mortality changes
620 to specific manufacturing industry or areas will be very difficult.

621

622 **Acknowledgments**

623 This study was supported by the National Natural Science Foundation of China (U21A6001) and
624 National Natural Science Foundation of China (42075044). The CESM project is supported
625 primarily by the National Science Foundation. The authors thank all the scientists, software
626 engineers, and administrators who contributed to the development of CESM 1.2.

627

628 **Conflict of Interest**

629 The authors declare no conflicts of interest relevant to this study.

630

631 **Code Availability Statement**

632 The code for the CESM 1.2 is publicly available at <https://www.cesm.ucar.edu/models/cesm1.2/>.
633 The code for post-processing and figure creation is available on request from the corresponding
634 author.

635

636 **Data Availability Statement**

637 The atmospheric GHGs concentrations of year 2020 come from NOAA (available at
638 <https://gml.noaa.gov/ccgg/trends/>). The air pollutant emission inventory comes from CESM1.2
639 and emissions input fields used to drive the simulations are downloaded automatically during the
640 model building process. Model results shown in this paper are available online
641 (<https://doi.org/10.5281/zenodo.6415030>).

642

643 The satellite-derived PM_{2.5} for assessing model results is available at
644 <https://sites.wustl.edu/acag/datasets/surface-pm2-5/>. The global gridded population data set is
645 available at <https://sedac.ciesin.columbia.edu/data/set/gpw-v4-population-count-rev11>. The
646 cause-specific mortalities for the five endpoints (GBD, 2019) are obtained from
647 <http://ghdx.healthdata.org/gbd-results-tool>. The VSL value for the individual countries or regions
648 is available at https://stats.oecd.org/Index.aspx?DataSetCode=EXP_PM2_5. Carbon dioxide
649 emissions per GDP are available at [https://www.climatewatchdata.org/ghg-](https://www.climatewatchdata.org/ghg-emissions?calculation=PER_GDP&end_year=2019®ions=CHN,IND,IDN§ors=total-fossil-fuels-and-cement&source=GCP&start_year=1960)
650 [emissions?calculation=PER_GDP&end_year=2019®ions=CHN,IND,IDN§ors=total-](https://www.climatewatchdata.org/ghg-emissions?calculation=PER_GDP&end_year=2019®ions=CHN,IND,IDN§ors=total-fossil-fuels-and-cement&source=GCP&start_year=1960)
651 [fossil-fuels-and-cement&source=GCP&start_year=1960](https://www.climatewatchdata.org/ghg-emissions?calculation=PER_GDP&end_year=2019®ions=CHN,IND,IDN§ors=total-fossil-fuels-and-cement&source=GCP&start_year=1960). National GDP in 2020 (\$ billions,
652 constant 2015; World Bank, 2020) is available at
653 <https://data.worldbank.org/indicator/NY.GDP.MKTP.KD>.

654

655

656 **References**

657 Andrew, R. M. (2020). Timely estimates of India's annual and monthly fossil CO₂ emissions. *Earth System Science*
658 *Data*, 12(4), 2411–2421. <https://doi.org/10.5194/essd-12-2411-2020>

659

660 Apte, J. S., Marshall, J. D., Cohen, A. J., & Brauer, M. (2015). Addressing Global Mortality from Ambient PM_{2.5}.
661 *Environmental Science & Technology*, 49(13), 8057-8066. <https://doi.org/10.1021/acs.est.5b01236>

662

663 Braathen, N.A., Lindhjem, H., Navrud, S., Directorate, E., & Pöyry, E. (2009). Valuing lives saved from
664 environmental, transport and health policies: A meta-analysis of stated preference studies.

665

666 BP. (2020). Statistical Review of World Energy [Dataset]. [https://www.bp.com/en/global/corporate/energy-](https://www.bp.com/en/global/corporate/energy-economics/statistical-review-of-world-energy.html)
667 [economics/statistical-review-of-world-energy.html](https://www.bp.com/en/global/corporate/energy-economics/statistical-review-of-world-energy.html)

668

669 Brauer, M., Freedman, G., Frostad, J., van Donkelaar, A., Martin, R. V., Dentener, F., et al. (2016). Ambient Air
670 Pollution Exposure Estimation for the Global Burden of Disease 2013. *Environmental Science & Technology*, 50(1),
671 79–88. <https://doi.org/10.1021/acs.est.5b03709>

672

673 Burnett, R. T., Pope, C. A. 3rd, Ezzati, M., Olives, C., Lim, S. S., Mehta, S., et al. (2014). An integrated risk
674 function for estimating the global burden of disease attributable to ambient fine particulate matter exposure.
675 *Environmental Health Perspectives*, 122, 397–403. <https://doi.org/10.1289/ehp.1307049>

676

677 Center for International Earth Science Information Network - CIESIN - Columbia University. (2018). Gridded
678 Population of the World, Version 4 (GPWv4): Population Count, Revision 11 [Dataset]. Palisades, NY: NASA
679 Socioeconomic Data and Applications Center (SEDAC). <https://doi.org/10.7927/H4JW8BX5>.

680

681 Chowdhury, S., & Dey, S. (2016), Cause-specific premature death from ambient PM_{2.5} exposure in India: estimate
682 adjusted for baseline mortality. *Environment International*, *91*, 283–290.
683 <https://doi.org/10.1016/j.envint.2016.03.004>

684

685 Cohen, A. J., Anderson, H. R., Ostro, B., Pandey K. D., Krzyzanowski, M., Künzli, N., et al. (2004). Urban air
686 pollution. In Ezzati M., Lopez A. D., Rodgers A., & Murray C. J.L. (Eds.) *Comparative Quantification of Health*
687 *Risks: Global and Regional Burden of Disease Attributable to Selected Major Risk Factors* (pp. 1353-1434).
688 Geneva: World Health Organization.

689

690 van Donkelaar, A., Hammer, M. S., Bindle, L., Brauer, M., Brook, J. R., Garay, M. J., et al. (2021). Monthly Global
691 Estimates of Fine Particulate Matter and Their Uncertainty. *Environmental Science & Technology*, *55*(22), 15287-
692 15300. <https://doi.org/10.1021/acs.est.1c05309>

693

694 Fernandes, N. (2020). Economic effects of coronavirus outbreak (COVID-19) on the world economy. *IESE Business*
695 *School Working Paper No. WP-1240-E*. <https://doi.org/10.2139/ssrn.3557504>

696

697 Sherman, E. (2020). 94% of the Fortune 1000 are seeing coronavirus supply chain disruptions: Report. *Fortune*.
698 <https://fortune.com/2020/02/21/fortune-1000-coronavirus-china-supply-chain-impact/>

699

700 Free, C., & Hecimovic, A. (2021). Global supply chains after COVID-19: the end of the road for neoliberal
701 globalisation? *Accounting, Auditing & Accountability Journal*, *34*(1), 58-84. [https://doi.org/10.1108/AAAJ-06-](https://doi.org/10.1108/AAAJ-06-2020-4634)
702 [2020-4634](https://doi.org/10.1108/AAAJ-06-2020-4634)

703

704 GBD. (2019). Global Burden of Disease Study 2019 Results [Dataset]. Institute for Health Metrics and Evaluation,
705 Seattle, United States. <http://ghdx.healthdata.org/gbd-results-tool>

706

707 Giannadaki, D., Giannakis, E., Pozzer, A., & Lelieveld, J. (2018). Estimating health and economic benefits of
708 reductions in air pollution from agriculture. *Science of the Total Environment*, *622-623*, 1304-1316.
709 <https://doi.org/10.1016/j.scitotenv.2017.12.064>

710

711 Giannadaki, D., Lelieveld, J., & Pozzer, A. (2016). Implementing the US air quality standard for PM_{2.5} worldwide
712 can prevent millions of premature deaths per year. *Environmental health*, *15*(1), 88. [https://doi.org/10.1186/s12940-](https://doi.org/10.1186/s12940-016-0170-8)
713 [016-0170-8](https://doi.org/10.1186/s12940-016-0170-8)

714
715 Global Burden of Disease Collaborative Network. (2013). Global Burden of Disease Study 2010 (GBD 2010) -
716 Ambient Air Pollution Risk Model 1990 – 2010 [Dataset]. Seattle, United States of America: Institute for Health
717 Metrics and Evaluation (IHME). <https://doi.org/10.6069/H0RR-H438>
718
719 Global Modeling and Assimilation Office (GMAO). (2015). MERRA-2 tavgM_2d_aer_Nx: 2d, Monthly mean,
720 Time-averaged, Single-Level, Assimilation, Aerosol Diagnostics V5.12.4 [Dataset]. Greenbelt, MD, USA, Goddard
721 Earth Sciences Data and Information Services Center (GES DISC). <https://doi.org/10.5067/FH9A0MLJPC7N>
722
723 Guan, D., Wang, D., Hallegatte, S., Davis, S. J., Huo, J., Li, s., *et al.* (2020). Global supply-chain effects of COVID-
724 19 control measures. *Nature Human Behaviour*, 4, 577–587. <https://doi.org/10.1038/s41562-020-0896-8>
725
726 Hayakawa, K., & Mukunoki, H. (2021). Impacts of COVID-19 on Global Value Chains. *The Developing*
727 *Economies*, 59, 154-177. <https://doi.org/10.1111/deve.12275>
728
729 Hedwall, M. (2020). The ongoing impact of COVID-19 on global supply chains. *World Economic Forum*.
730 <https://www.weforum.org/agenda/2020/06/ongoing-impact-covid-19-global-supply-chains/>
731
732 Hurrell, J. W., Holland, M. M., Gent, P. R., Ghan, S., Kay, J. E., Kushner, P. J., *et al.* (2013). The community earth
733 system model: A framework for collaborative research. *Bulletin of the American Meteorological Society*, 94(9),
734 1339–1360. <https://doi.org/10.1175/BAMS-D-12-00121.1>
735
736 IPCC. (2006). 2006 IPCC Guidelines for National Greenhouse Gas Inventories, Prepared by the National
737 Greenhouse Gas Inventories Programme. In Eggleston, H. S., Buendia, L., Miwa, K., Ngara, T., & Tanabe, K.
738 (Eds.). Japan: Institute for Global Environmental Strategies (IGES).
739
740 IPCC. (2014). Climate Change 2014: Synthesis Report. Contribution of Working Groups I, II and III to the Fifth
741 Assessment Report of the Intergovernmental Panel on Climate Change [Core Writing Team. In Pachauri, R. K., &
742 Meyer, L. A. (Eds.)]. IPCC, Geneva, Switzerland, 151 pp.
743
744 Ivanov, D. (2020). Predicting the impacts of epidemic outbreaks on global supply chains: A simulation-based
745 analysis on the coronavirus outbreak (COVID-19/SARS-CoV-2) case. *Transportation Research Part E: Logistics*
746 *and Transportation Review*, 136. <https://doi.org/10.1016/j.tre.2020.101922>.
747
748 Lelieveld, J., Barlas, C., Giannadaki, D., Pozzer, A. (2013). Model calculated global, regional and megacity
749 premature mortality due to air pollution. *Atmospheric Chemistry and Physics*, 13, 7023–7037.
750 <https://doi.org/10.5194/acp-13-7023-2013>

751
752 Lin, J. & Lanng, C. (2020). Here's how global supply chains will change after COVID-19. *World Economic Forum*.
753 <https://www.weforum.org/agenda/2020/05/this-is-what-global-supply-chains-will-look-like-after-covid-19/>
754
755 Lin, J., Pan, D., Davis, S. J., Zhang, Q., He, K., Wang, C., et al. (2014). China's international trade and air pollution
756 in the United States. *Proceedings of the National Academy of Sciences of the United States of America*, 111(5),
757 1736-1741. <https://doi.org/10.1073/pnas.1312860111>
758
759 Lin, J., Tong, D., Davis, S., Ni, R., Tan, X., Pan, D., et al. (2016). Global climate forcing of aerosols embodied in
760 international trade. *Nature Geoscience*, 9, 790–794. <https://doi.org/10.1038/ngeo2798>
761
762 Liu, X., Easter, R. C., Ghan, S. J., Zaveri, R., Rasch, P., Shi, X., et al. (2012). Toward a minimal representation of
763 aerosols in climate models: Description and evaluation in the Community Atmosphere Model CAM5. *Geoscientific*
764 *Model Development*, 5, 709–739. <https://doi.org/10.5194/gmd-5-709-2012>
765
766 Liu, Y., Lee, J. M., & Lee, C. (2020), The challenges and opportunities of a global health crisis: the management
767 and business implications of COVID-19 from an Asian perspective. *Asian Business & Management*, 19(3), 277-297.
768 <https://doi.org/10.1057/s41291-020-00119-x>
769
770 Lu, X., Lin, C., Li, Y., Yao, T., Fung, J. C., & Lau, A. K. (2017). Assessment of health burden caused by particulate
771 matter in southern China using high-resolution satellite observation. *Environment International*, 98, 160-170.
772 <https://doi.org/10.1016/j.envint.2016.11.002>
773
774 Maji, K. J., Ye, W.F., Arora, M., & Shiva Nagendra, S.M. (2018). PM_{2.5}-related health and economic loss
775 assessment for 338 Chinese cities. *Environment International*, 121, 392-403.
776 <https://doi.org/10.1016/j.envint.2018.09.024>
777
778 Moss, R. H., Edmonds, J. A., Hibbard, K. A., Manning, M. R., Rose, S. K., van Vuuren, D. P., et al. (2010). The
779 next generation of scenarios for climate change research and assessment. *Nature*, 463, 747–756.
780 <https://doi.org/10.1038/nature08823>
781
782 NBSC. (2017). China Statistical Yearbook 2017 [Dataset]. National Bureau of Statistical of China.
783 <http://www.stats.gov.cn/tjsj/ndsj/2017/indexeh.htm>
784
785 Neale, R. B., Gettelman, A., Park, S., Conley, A. J., Kinnison, D., Marsh, D., et al. (2012). Description of the NCAR
786 community atmosphere model (CAM 5.0). NCAR Technical Note NCAR/TN-486+ STR.
787

788 Nicola, M., Alsafi, Z., Sohrabi, C., Kerwan, A., Al-Jabir, A., Iosifidis, C., et al. (2020). The socio-economic
789 implications of the coronavirus pandemic (COVID-19): A review. *International journal of surgery (London,*
790 *England)*, 78, 185–193. <https://doi.org/10.1016/j.ijssu.2020.04.018>
791

792 OECD. (2012). *Mortality Risk Valuation in Environment, Health and Transport Policies*. Paris: OECD Publishing.
793 <https://doi.org/10.1787/9789264130807-en>
794

795 OECD. (2014). *The Cost of Air Pollution: Health Impacts of Road Transport*. Paris: OECD Publishing.
796 <https://doi.org/10.1787/9789264210448-en>
797

798 OECD. (2017). *The Rising Cost of Ambient Air Pollution thus far in the 21st Century: Results from the BRIICS and*
799 *the OECD Countries*. Paris: OECD Publishing. <http://dx.doi.org/10.1787/d1b2b844-en>
800

801 OECD Statistics. (2020). *Mortality, morbidity and welfare cost from exposure to environment-related risks*
802 [Dataset]. https://stats.oecd.org/Index.aspx?DataSetCode=EXP_PM2_5
803

804 Pope, C. A. III, Burnett, R. T., Krewski, D., Jerrett, M., Shi, Y., Calle, E. E., et al. (2009). Cardiovascular mortality
805 and exposure to fine particulate matter from air pollution and cigarette smoke: shape of the exposure-response
806 relationship. *Circulation*, 120, 941–948. <https://doi.org/10.1161/CIRCULATIONAHA.109.857888>
807

808 Pope, C. A. III, Burnett, R. T., Turner, M. C., Cohen, A., Krewski, D., Jerrett, M. et al. (2011). Lung cancer and
809 cardiovascular disease mortality associated with particulate matter exposure from ambient air pollution and cigarette
810 smoke: shape of the exposure–response relationships. *Environmental Health Perspectives*, 119, 1616–1621.
811 <https://doi.org/10.1289/ehp.1103639>
812

813 Ran, Q., Lee, S. Y., Moore, J. C., Min, C., & Dong, W. (2021). Economic shock in a climate scenario and its impact
814 on surface temperatures. *Earth's Future*, 9, e2021EF002061. <https://doi.org/10.1029/2021EF002061>
815

816 Roman, H. A., Hammitt, J. K., Walsh, T. L., & Stieb, D. M. (2012). Expert elicitation of the value
817 per statistical life in an air pollution context. *Risk Analysis*, 32(12), 2133–2151. [https://](https://doi.org/10.1111/j.1539-6924.2012.01826.x)
818 doi.org/10.1111/j.1539-6924.2012.01826.x
819

820 Taylor, K. E., Stouffer, R. J., & Meehl, G. A. (2012). An overview of CMIP5 and the experiment design. *Bulletin of*
821 *the American Meteorological Society*, 93(4), 485–498. <https://doi.org/10.1175/BAMS-D-11-00094.1>
822

823 Textor, C., Schulz, M., Guibert, S., Kinne, S., Balkanski, Y., Bauer, S., et al. (2005). Analysis and quantification of
824 the diversities of aerosol life cycles within AeroCom. *Atmospheric Chemistry and Physics*, 6, 1777–1813.
825 <https://doi.org/10.5194/acp-6-1777-2006>
826

827 Wang, Q, Wang, J, He, MZ, Kinney, P.L., & Li, T. (2018). A county-level estimate of PM_{2.5} related chronic
828 mortality risk in China based on multi-model exposure data. *Environment International*, 110, 105-112.
829 <https://doi.org/10.1016/j.envint.2017.10.015>
830

831 Wei, T., Dong, W., Moore, J., Yan, Q., Song, Y., Yang, Z., et al. (2016). Quantitative Estimation of the Climatic
832 Effects of Carbon Transferred by International Trade. *Scientific Reports*, 6, 28046.
833 <https://doi.org/10.1038/srep28046>
834

835 World Bank. (2020). GDP (constant 2015 US\$) [Dataset]. <https://data.worldbank.org/indicator/NY.GDP.MKTP.KD>
836

837 Zhang, Q., Jiang, X., Tong, D., Davis, S. J., Zhao, H., Geng, G., et al. (2017). Transboundary health impacts of
838 transported global air pollution and international trade. *Nature* 543, 705–709. <https://doi.org/10.1038/nature21712>